

Combustion Analysis by Radical Intensity Measurement and Instantaneous Image in a Constant-volume Chamber

C-H.Jeon, S-J.Choi, H-J. Park and Y-J.Chang*

*Department of Mechanical & Precision Engineering
Faculty of Engineering
Pusan National University
30 Changjeon-Dong, Kumjeong-Ku, Pusan 609-735
Korea*

* *Pusan National University*

ABSTRACT

In these days, air pollution problems by automobile exhaust gas become serious, and it is demanded to know precisely flame propagation characteristics which are directly associated with the mechanism of pollutant formation in the exhaust gas. To clarify the laminar flame propagation process and combustion radical characteristics of methane-air premixtures in a closed cylindrical combustion chamber, experimental approaches are carried out in this study.

Two measuring systems are used in this experiments such as flame propagation measurement by pressure transducer, ion probe, schlieren device and combustion radical intensity measurement by interference filter, dichroic mirror, etc.

In combustion radical study, one of the purposes is to determine correlation between local radicals intensity of CH^* , C_2^* , OH^* in methane/air mixture along with radial direction. Another is proposed estimation equation of the equivalence ratio by the ratio of average CH^* to C_2^* radicals intensity.

Various results are presented to illustrate the effect of equivalence ratio and initial condition on radical production characteristics and correlation. The proposed equations of two kinds such as continuous flame type and intermittent flame type are evaluated by the ratio of radical intensities of two different wavelengths, 431nm(CH^* radical) and 517nm(C_2^* radical). The equation for continuous flame type is agreed with actual equivalence ratio within 10% errors during 10ms around radical peaks. The estimation data show that the equivalence ratio was higher at the beginning of combustion and gradually decreased.

1. INTRODUCTION

Recently, flame diagnostics and measuring techniques of combustion using flame spectra method paid attention such as mixing ratio, concentration of molecules and radicals, reaction ratio, etc.⁽¹⁾ Color of flame emissions is determined by every kind of combustion radicals which involved various information according to combustion condition, namely equivalence ratio, flame temperature and combustion pattern. Therefore the study of emissions from flames forms an newly important facet of combustion analysis, with implications for future combustion measuring strategy.

Much works has been attempted regarding luminous emission from burner flame and spark ignition engines.⁽²⁾⁻⁽³⁾ Each combustion processes consist of a

propagating flame and luminous emission. A spark plug integrated optical combustion sensor which inserted quartz glass optical fiber through the center, can be used for detecting spark timing and knocking from engine flame.⁽⁴⁾ And the emission spectra from engine flames, the radiation at the end of each flame, the crank angle of a peak in radiant emission for air-fuel ratio and spark advance, and air-fuel ratio can all be determined. Measurement for excess air ratio which used radical emission from burner flame, has been reported using emission intensity ratio of CH^* , C_2^* radical.⁽⁶⁾

Along these lines, the present study examines the relationship between radical characteristics of OH^* , CH^* , C_2^* and flame development in quiescent methane/air mixtures based on equivalence ratio, flame speed and pressure using ion current probe and capacitor discharge ignition system(CDI). The present investigation was considered necessary prior to attempting correlation studies in a high turbulence, spark ignition engine in order to allow a reduction of the parameters of interest and better focussing on the lean burn limit where the problems of misfire and increased cyclic variations emission mechanism are still unresolved.

2. EXPERIMENTAL SYSTEM

2.1 Schematic Configuration

Methane/air were premixed into a mixture tank where their equivalence ratio was determined based on their partial pressures measured by a diaphragm pressure transducer (methane) and a digital pressure gauge(air) at total mixture of up to 9 bars. The mixture was then introduced into a constant-volume combustion chamber through a high-pressure line equipped with a pressure regulator to adjust the initial chamber pressure and a solenoid valve to control the swirling flow entering the chamber through a tangential port.

Fig.1 shows a schematic diagram of the cylindrical combustion chamber. Combustion chamber of duralumin has a 70mm diameter, a 34mm depth and a volume of 130cm³. The chamber contains a pair of parallel fused silica windows of 20mm thickness through which optical access can be provided for flame-spectra techniques. Two plate heaters, plugged in the walls of the chamber and coupled to a J-type temperature controller, allowed the temperature of chamber to kept constant at various levels up to 403.2K in order to change mixture temperature.

Under quiescent flow conditions, the mixture was allowed enough time to decay swirling completely in the chamber. The mixture was ignited using capacitor discharge ignition system (CDI) with variable ignition energy and elongated spark plugs which inserted steel rod, 2mm diameter to locate spark point at center of chamber.

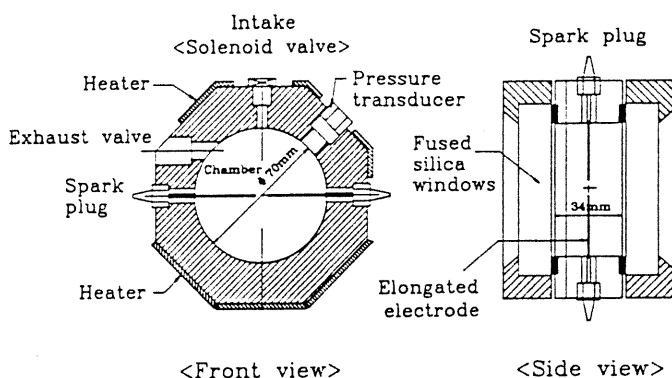


Fig. 1 Schematic of constant-volume combustion chamber

2.2 Experimental Techniques

This experimental apparatus consisted of the following four parts; optical system for measuring local and average combustion radical intensity, flame speed measuring system, combustion pressure measurement for calculate mass burning rate, and instantaneous image acquisition system - schlieren and radical CCD image.

Measurement of radical intensity

The effective information of a reaction area and a reaction mechanism is obtained by measuring emission intensity of radical such as OH^* , CH^* and C_2^* . As radicals emit intrinsic lights, the kinds and distributions of radicals can be estimated by measuring intensity distribution of radical's intrinsic emission.

In hydrocarbon's flame, C_2^* radical generate in the early decomposition process which are produced by cool and dark flame in the preliminary reaction of fuel prior to ignition, and then CH^* radical generates.⁽⁵⁾ C_2^* dominate in rich mixture area and CH^* in the lean area. Swan band (516.5nm) is typical in C_2^* . The Three bands of 314.3, 390.0 and 431.5nm are observed in CH^* , 516.5nm in C_2^* and 431.5nm in CH^* have been chosen because of visible radiation.

Fig. 2 shows a optical arrangement for measuring radical intensity. As shown in Fig. 2, lightened flame luminosity of local area was collected through a fused silica window, condensed by a quartz lens, then the emission was divided into each of the branched optical passage by dichroic mirror. The transferred light emission through each of the branched passages was passed through a respective band pass filter which is transparent only for a predetermined range of wave length.

The intensity of the screened light emission of PM tube was converted to an electric signal by a PM amplified and recorded on a data acquisition board. Table.1 summarizes filter and mirror characteristics of OH^* , CH^* , C_2^* radicals. The discrepancy between measuring radicals and filter central wavelength was involved in band widths.

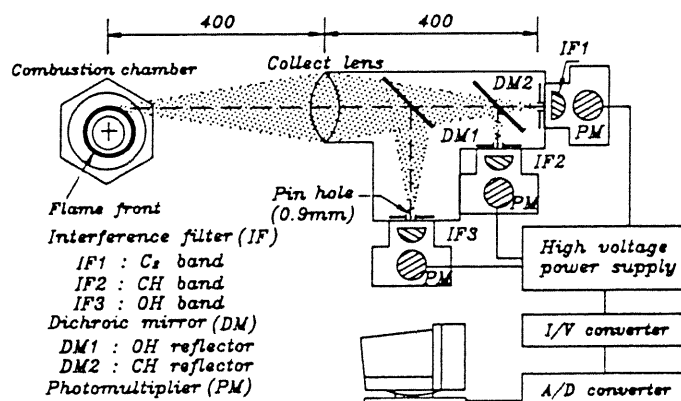


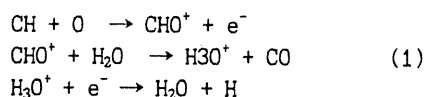
Fig. 2 Optics configuration to monitor local radical intensity of combustion radical

Table. 1 Specification of filter and dichroic mirror

	Radical species	Observed spectrum	Wave length λ (nm)	Band width λ (nm)	Trans. rate
Filter	CH^*	431 nm	432.3	1.2	49.2%
	C_2^*	517 nm	515.5	1.6	65.0%
	OH^*	309 nm	310.1	12	35.0%
Dichr. mirror	CH^*	431 nm	CH^* Reflector		99.0%
	OH^*	309 nm	OH^* Reflector		97.0%

Measurement of flame speed

The chemi-ionization in hydrocarbon-air flames is extra-equilibrium and is associated principally with the flame front kinetic reactions



Ionization from these reaction is rapidly decayed by recombination, the maximum ionisation occurs in the region of comparely narrow band near flame reaction zone. An electrical potential applied to each of the two ionization probe which was connected to an independent circuits and immersed in a flame creates current of positive ions. The arrival of the flame front at each probe was indicated by a rapidly increasing current pulse. The present study employed two identical Ni-100% probes of 0.2mm diameter, 1mm width and 5 point from center to the wall of chamber both directions. As the probe current might be measured in the nanoamp, it was vital to ensure good insulation and avoid both earth loops and electromagnetic interference. The common earth terminal was the combustion chamber itself and all leads were screened with coaxial, low noise cables. However, spark ignition interference could not be eliminated entirely, but it was returned to good use in recording the spark timing and triggering the oscilloscope. It was then assumed that the probe were aligned orthogonally to the direction of flame propagation and the flame speed was given by the distance apart of the probes divided by this time interval. Because this method is a cross-check

measurement, the accuracy of the system is consistent for highly irregular flame shapes since we can remove unsymmetrical flame propagation by using both direction check of flame propagation. Moreover, in the present case, the error is expected to be negligibly small since the flame according to a previous schlieren visualization study is symmetric around chamber axis and an average is obtained over at least five single shot experiments.

Measurement of chamber pressure

The instantaneous pressure development in the combustion chamber was measured by a piezoelectric pressure transducer (AVL QC31) connected to a charge amplifier. Mass fraction burned and mass burning rate (MBR) were calculated using assumption which maximum pressure is complete combustion condition. Based on the measured pressure trace, a range of characteristic values were estimated and analysed to describe the flame kernel initiation and flame development.

- (a) peak pressure, P_{max} and time (total combustion duration)
- (b) time from 10% to 90% of the mass burned
 $t_{90} - t_{10} = t_{91}$

Visualization - Schlieren and radical CCD image

Schlieren high speed photography were taken to define details of the flow and density fields through the flame propagation. The effect information of a reaction area and a reaction mechanism is obtained by measuring emission intensity distribution of radicals. Instantaneous radical images (shutter time 100ns) of flame is very weak. Therefore CCD and high speed gated image intensifier is used. Because the weak luminous intensity of the flames prohibits to use any high speed camera and a very short exposure time is not sufficient for getting a clear image on a film.

2.3 Experimental Conditions and Procedure

After adjusting initial mixture pressure, temperature, equivalence ratio, they were ignited. The electrical characteristics of ignition system were ignored under enough spark energy which minimum ignition energy is a few mJoule in this experimental ranges. Then radical intensity were monitored simultaneously in order to investigate the correlation between radical characteristics of emission and flame development. Schlieren device and ion probes measured local and average flame speed. Each experimental apparatus used with combustion pressure.

Table. 2 Experimental Conditions

Parameter	Condition
Pressure, P_1 (MPa)	0.08, 0.24, 0.40 (gauge)
Equivalence Ratio, ϕ	0.8, 0.9, 1.0, 1.1, 1.2
Temperature, T (K)	313.2, 353.2, 403.2

The experimental condition are summarized in Table 2. In our experimental conditions, we could consider three factor to be influenced flame propagation - equivalence ratio, initial pressure and temperature.

3. RESULT AND DISCUSSION

Flame Radius and Mass Burning Rate

Fig.3 shows the trace of flame radius in high speed schlieren photo at each equivalence ratio condition. The growth speed of flame radius are determined before 3ms in the range of equivalence ratio 1.0 above, then flame propagate constant velocity. The leaner methane-air premixture becomes, the more slow flame growth speed.

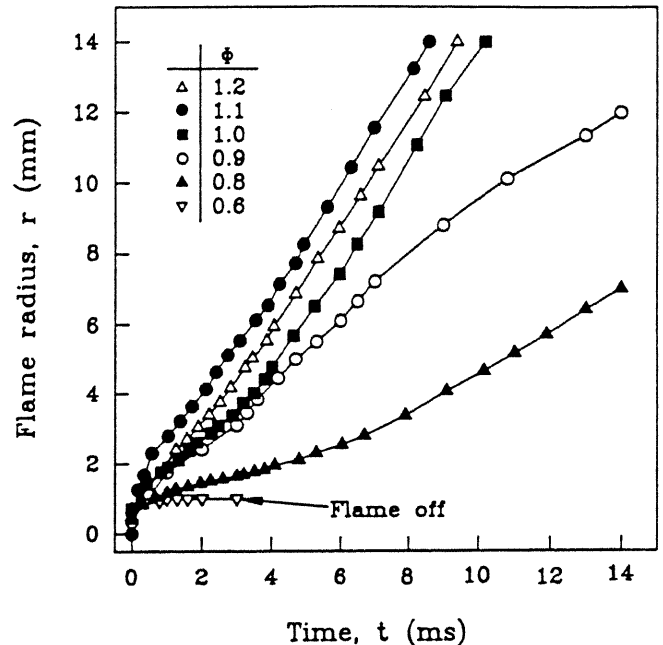


Fig.3 Effect of equivalence ratio on the flame propagation radius ($P_i=0.24\text{MPa}$, $T_i=313.2\text{K}$)

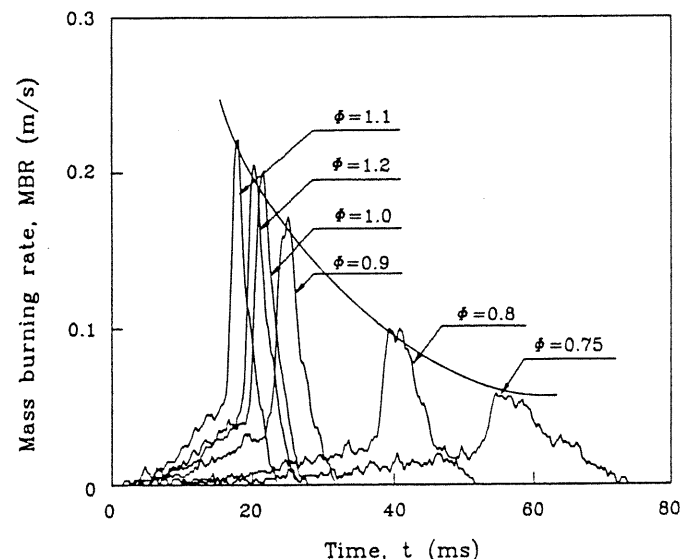


Fig. 4 Effect of equivalence ratio on the mass burning rate ($P_i=0.24\text{MPa}$, $T_i=313.2\text{K}$)

From combustion pressure traces the the mass burning rate (MBR) was determined by the Lewis and Von Elbe⁽⁶⁾ result using Lagrangian Interpolation methods.

Fig.4 shows the results for mass fraction burned

with different mixture strength, 0.75-1.2. It can be seen that an increase in a time to burn 100% of the mixture(t_{pmax}). It can also be seen that the initial burning rate is much higher for the rich mixture condition. The time to mixture mass burning rate include information both initial pressure and temperature. The effect of the initial mixture pressure and temperature based on MBR get longer with high initial pressure. But mixture is a high initial temperature, time to MBR becomes shorter.

Flame Speed

Fig.5 shows results obtained with both direction ion probe method of the flame propagation speed along the chamber axis as a function of initial mixture pressure, temperature and equivalence ratio. Since the flow is quiescent, the observed variation of flame speed with the thermodynamic properties of the mixture is due to variation of the laminar burning velocity and of the electrical characteristics as affected by mixture pressure and, less so, temperature.

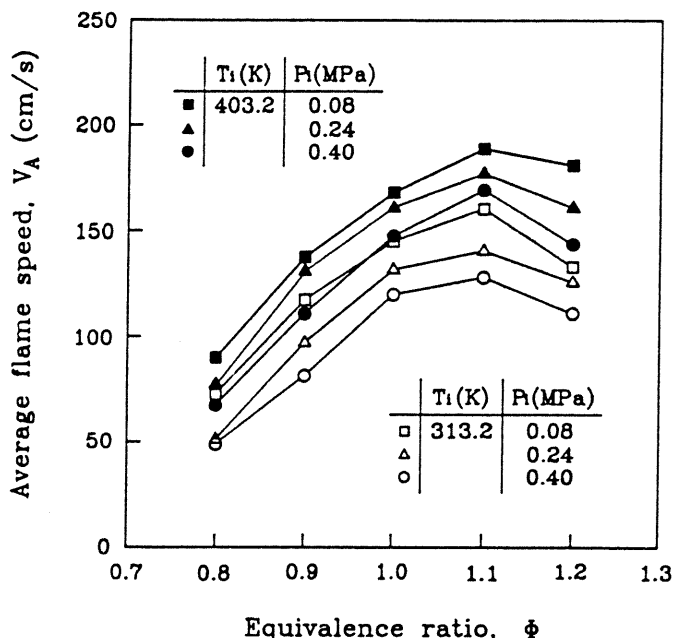


Fig. 5 Effect of equivalence ratio on average flame speed

As shown in Fig.5, the peak flame propagation speed decrease at higher initial mixture pressure and lower initial mixture temperature and is maximum at mixture equivalence ratio between 1.0 and 1.1. The effect of mixture pressure on flame speed follows that on burning velocity and confirms that, as the pressure increases, the spatial variation of the flame speed becomes more uniform. Similarly to the effect of mixture pressure on burning velocity a higher initial temperature gives rise to a higher flame speed nearly propagational to the temperature square. In addition, as the mixture becomes leaner, the spatial distribution of the flame speed becomes none uniform and peaks at equivalence ratio between 1.0 and 1.1 in agreement with the results in the literature which showed maximum laminar burning velocities at slightly rich condition, 1.05-1.1.⁽⁶⁾

Flame development is described as the time that it

takes for 10% of the mixture to burn(t_{10}), which is indicative of the post flame initiation process, the time for 90% of the mixture to burn(t_{90}) and the time to peak pressure(t_{pmax}) which represents total burn duration.

Comparison between Fig.4 and Fig.5 shows that there is good correlation between the pressure development and flame propagation speeds. As expected, combustion duration gets longer with higher initial pressure, and lower initial temperature. Flame propagation speed was found to be lower for higher initial mixture pressure.

Radical Characteristics

Fig.6 shows the OH^* , CH^* , C_2^* radical signal output at each local point, $r=10, 20, 30$ mm from center.

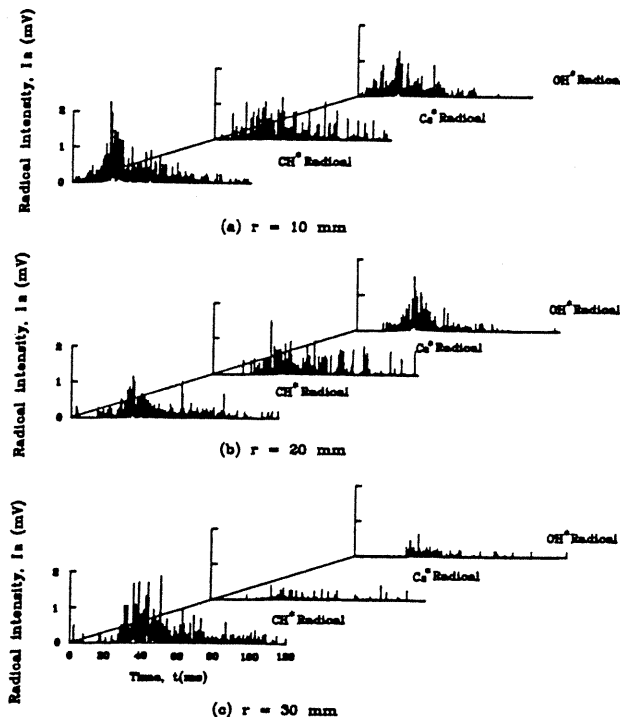


Fig. 6 Each radical signals along the measurement position ($P_i=0.08$ MPa, $T_i=313.2$ K)

Fig.7 shows cross-correlation along the position of center, CH^* radical relative to each positions, OH^* radical. This attempts calculation of flame speed by local radical characteristic deduced from peak delay time(Δr) relate to same interval($\Delta r=10$ mm). Flame speed($\Delta r/\Delta \tau$) is 176.64, 171.82cm/s near the stoichiometric range, same as ion probe data with in 5% difference.

Equivalence Ratio Characteristics

H.Itoh, etal⁽⁷⁾ reported that equivalence ratio of butane-air premixed flame strongly relate intensity ratio of CH^* , C_2^* radical. In present study, equivalence ratio can be calculated by intensity ratio of CH^* , C_2^* radical as similar methods.

Fig.8 shows calculation modes to find best time interval which equivalence ratio is proportional to average radical intensity. Then proportional equation express within this experiment range. Equivalence ratio using CH^* , C_2^* radical data is calculated by following equation.

$$\text{Equi. Ratio}(\phi) = C_1 \times \ln(ICH^*/IC_2^*) + C_2 \quad (2)$$

where C_1, C_2 is experimental device constant.

Fig.9 shows the variation of C_1, C_2 along the each modes. Midpoint peak mode is calculated relative exactly equivalence ratio within 10ms from peak center. In present work C_1, C_2 is determined, $C_1=0.4526, C_2=0.5677$.

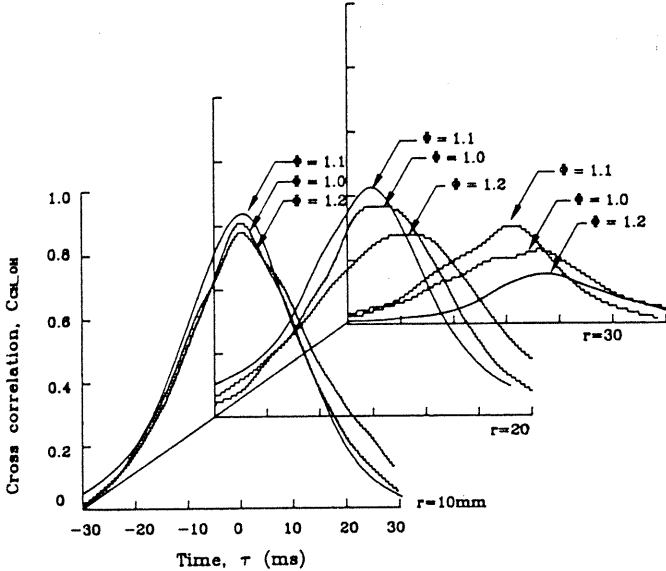


Fig. 7 Cross-correlation function between CH^*, OH^* radical ($P_i=0.24MPa, T_i=313.2K$)

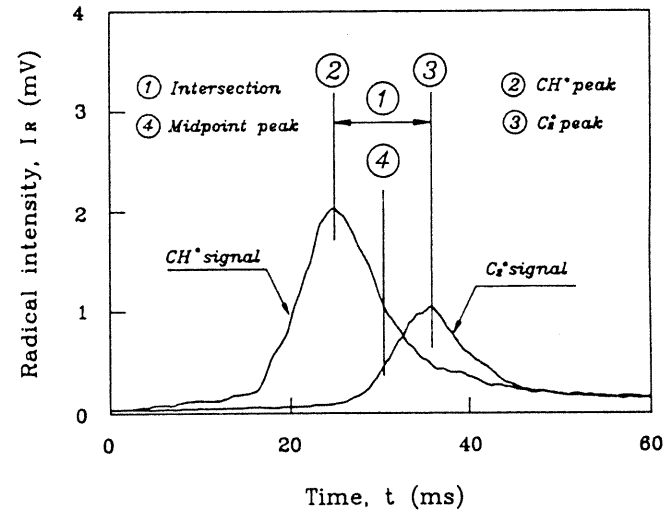


Fig. 8 Calculation modes of radical intensity

Fig.10 show change of estimated equivalence ratio along to average radical intensity. As shown in Fig.10, it show good agreement near peak radicals, but calculate as rich before 10ms from peak and lean after 10ms from peak.

Another method for calculation of equivalence ratio is intermittent flame type. A radical intensity time signal consider information to analyze four factor : CH^*, OH^* radical luminous amount (I_{CH, C_2}), luminous time(T_{CH, C_2}), pressure and temperature factor. A radical time signal have unique each factor. Equivalence ratio is described combination of these factors.

If radical luminous and time factor is proportional to equivalence ratio, following equation express within this experiment range.

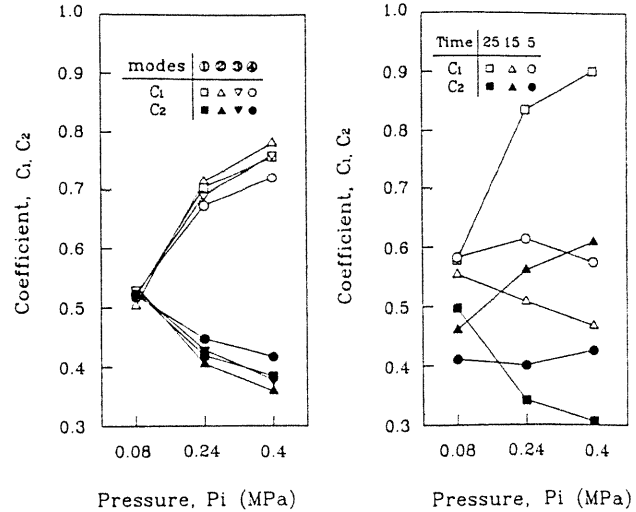


Fig. 9 Effect of initial pressure on coefficient C_1, C_2

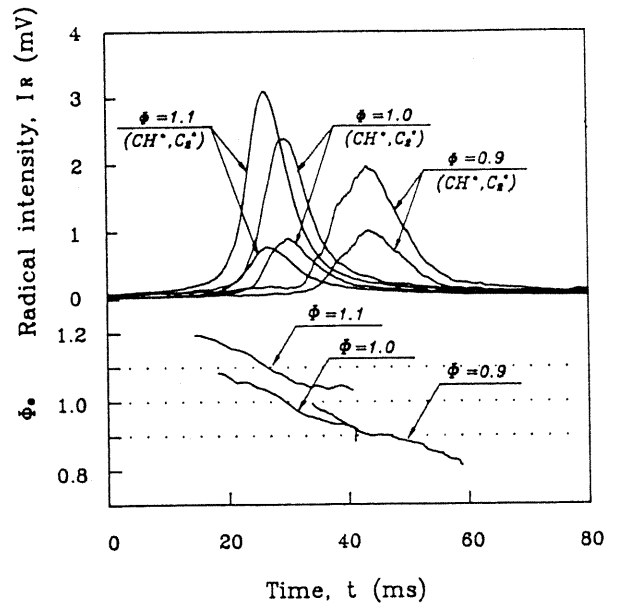


Fig. 10 Equivalence ratio change to calculation time ($P_i=0.24MPa, T_i=353.2K$)

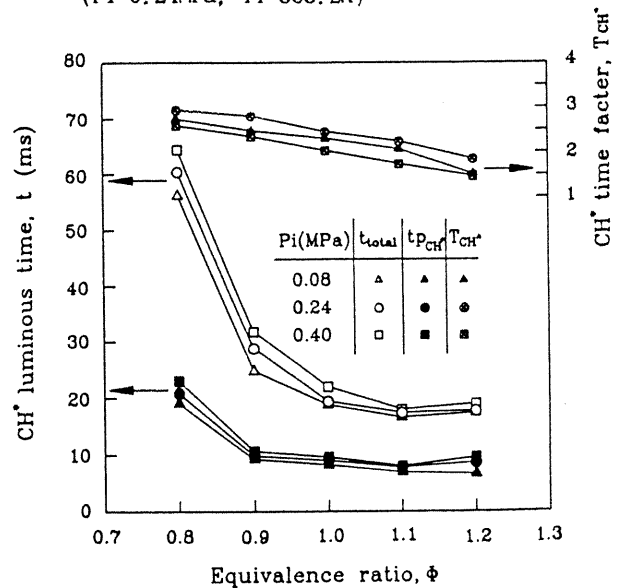


Fig.11 Effect of equivalence ratio on CH^* time factor

Therefore coefficient of equation means slope which appear importance role of each factor.

$$\phi = C_1 + (C_2 \times I_{CD}) + (C_3 \times I_{CD}) + (C_4 \times T_{CD}) + (C_5 \times T_{CD}) \quad (3)$$

where $C_1 \dots C_5$ is experimental device constants.

In present work, $C_1 = -0.928$, $C_2 = 1.535$, $C_3 = -0.716$, $C_4 = -0.667$, $C_5 = -0.501$. Luminous factors take place opposite tendency to luminous time factor along equivalence ratio. Fig. 11 shows the variation of CH^* time factor along equivalence ratio.

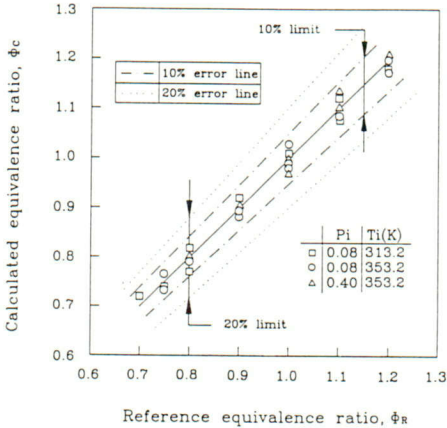


Fig. 12 Relation between calculated ϕ_c and reference ϕ_R

Fig 12 shows correlation between actual equivalence ratio (ϕ_R) and calculated equivalence ratio (ϕ_c) by equation (3). Good agreement between actual equivalence ratio (ϕ_R) and calculated equivalence ratio (ϕ_c) is obtained for the equation of intermittent flame type within $\pm 4.1\%$ error.

Instantaneous Radical Image

Fig.13 shows schlieren photographs, pseudo colored CCD images and CH^* radical images of methane-air premixture at equivalence ratio 1.0. The pseudo colored images distinguish ten colors per 10 grey levels which eliminate background image. Comparing flame radius of the pseudo colored image and the schlieren photo, we know that the flame radius of pseudo colored image is larger than that of the schlieren photography. But, we can find that flame front of schlieren photo is nearly agreed with the peak of radical luminous intensity (white color of pseudo colored CCD image).

4. CONCLUSIONS

The Relationship between combustion radical characteristics and flame development was investigated for quiescent methane/air mixtures using a Capacitor Discharge Ignition System (CDI). The parameters examined included the initial mixture pressure, temperature and equivalence ratio.

1) Lower initial mixture pressure, higher initial

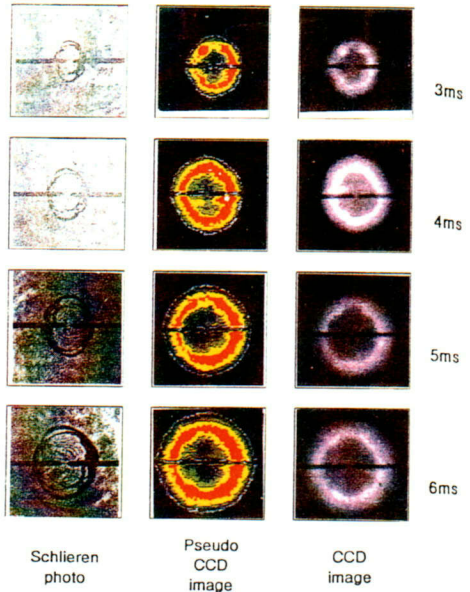


Fig. 13 Comparison between schlieren photo, pseudo CCD image and CCD image ($\phi = 1.0$)

temperature gave rise to faster flame propagation.

2) Although experimental limits is comparably narrow from 0.8 to 1.2 in equivalence ratio, estimation equation of two type using intensity ratio CH^*/C_2^* was found to be good within 10ms.

3) Flame radius of pseudo colored radical image is larger than that of the schlieren photography. But, flame front of schlieren photo is nearly agreed with the peak of radical luminous intensity.

REFERENCE

- (1) Y.Miztani, "Visualization and Image Analysis of Combustion Field", JSME Int. J. Series II, Vol 32, No.1, PP.1-10, 1989.
- (2) T.Sasayama, et al., "Recent Development of Optical Fiber Sensors for Automotive Use", SPIE Vol. 840, 1987.
- (3) E.Day, et al., "Start of Combustion Sensor", SAE Paper 890484, 1989.
- (4) Y.Ohyama, et al., "Study on Optical Combustion Sensor for Spark Ignition Engine", COMODIA 90, PP.359-364, 1990.
- (6) Lewis, B.L and von Elbe, G., "Combustion, Flames and Explosions of Gases, Academic Press, 1961.
- (7) H.Itoh, Y.Hommo, Jae-ik Song and T.gomi, "An Instantaneous Measuring Method of Air-Fuel Ratio by Luminous Intensity of Radical", JSME(B), Vol.52, No.481, pp.2219-2230, 1988.